5⊘CellPress

Contents lists available at ScienceDirect

# Heliyon

journal homepage: www.cell.com/heliyon



#### Research article

Prognostic model based on M2 macrophage-related signatures for predicting outcomes, enhancing risk stratification, and providing therapeutic insights in diffuse large B-cell lymphoma

Baoping Guo \*\*, Ying Duan, Hong Cen

Department of Hematology, Guangxi Medical University Cancer Hospital, Nanning, Guangxi, 530021, China

#### ARTICLE INFO

Keywords:
DLBCL
Immune
M2 macrophage
Prognostic model
Tumor microenvironment

#### ABSTRACT

*Purpose*: The tumor microenvironment (TME) in lymphoma is influenced by M2 macrophages. This research proposes an novel predictive model that leverages M2 macrophage-associated genes to categorize risk, forecast outcomes, and evaluate the immune profile in patients with newly diagnosed diffuse large B-cell lymphoma (DLBCL) undergoing R-CHOP therapy.

Methods: Gene expression data and clinical information from DLBCL patients were retrieved from The Cancer Genome Atlas (TCGA) and Gene Expression Omnibus (GEO) databases. Co-expressed genes linked to M2 macrophage in DLBCL were analyzed using CIBERSORT. Gene Ontology (GO) and Kyoto Encyclopedia of Genes and Genomes (KEGG) pathway analyses were conducted to explore associated signaling pathways. The M2 macrophage-related gene prognostic model was developed and validated using Cox and LASSO regression. Prognostic signature genes were verified by single-cell RNA-seq analysis.

Results: 92 M2 macrophage-related genes were identified based on bulk-seq data. MS4A4A, CCL13, LTB, CCL23, CCL18, XKR4, IL22RA2, and FOLR2 were used to construct the risk model. AUC values for 1-, 3-, and 5-year survival were 0.74, 0.72, and 0.72, respectively. High-risk patients demonstrated elevated immune scores and poorer overall survival. The high-risk subgroup also exhibited greater sensitivity to both chemotherapeutic agents and immune checkpoint inhibitors.

Conclusion: This study presents an accurate and reliable M2 macrophage-related risk model, enhancing understanding of distinct prognostic subsets in DLBCL. It offers potential novel drug options for future treatments.

## 1. Introduction

Diffuse large B-cell lymphoma (DLBCL) is one of the most commonly diagnosed forms of non-Hodgkin lymphoma, representing 30–40 % of all cases [1]. Although the incorporation of the anti-CD20 monoclonal antibody rituximab into chemotherapy has significantly improved DLBCL survival, the prognosis for DLBCL patients remains poor, necessitating the exploration of new

E-mail addresses: dr\_duran@126.com (B. Guo), cenhong981@gxmu.edu.cn (H. Cen).

<sup>\*</sup> Corresponding author. Department of Hematology, Guangxi Medical University Cancer Hospital, 71 Hedi Avenue, Nanning, Guangxi, 530021, China.

<sup>\*\*</sup> Corresponding author. Department of Hematology, Guangxi Medical University Cancer Hospital, 71 Hedi Avenue, Nanning, Guangxi, 530021, China

therapeutic targets [2,3]. Gene expression profiling studies of DLBCL biopsy specimens have revealed increased infiltration of macrophages into the DLBCL stroma [4]. Within the tumor microenvironment, macrophages exist in diverse polarized subtypes, with functional heterogeneity observed between M1 and M2 macrophages. However, the specific mechanisms underlying the impact of M2 macrophage infiltration on DLBCL pathogenesis remain unclear [5,6].

Expression of immune checkpoint genes in diffuse large B-cell lymphoma (DLBCL) exhibits heterogeneity. PD-1/PD-L1 blockade emerges as a potential therapeutic strategy for patients with refractory or relapsed DLBCL [7]. The prognostic and predictive biomarkers associated with immune infiltration and the expression of PD-1, PD-L1, PD-L2, and CTLA-4 in DLBCL samples remain poorly defined.

The role of macrophages in the tumor microenvironment has been a subject of controversy [8]. In the classical model, macrophages are classified into M1 and M2 subtypes, each characterized by distinct activation mechanisms and effector functions [9]. M1 polarization is linked to macrophage-mediated tissue damage and tumor cell killing, whereas M2 polarization is believed to support tumor growth by suppressing immune responses and promoting angiogenesis [10]. A high abundance of tumor-associated macrophages (TAMs) has been associated with poor prognosis in DLBCL patients not treated with rituximab [11–14]. Conversely, high TAM infiltration has been associated with a favorable outcome in patients treated with rituximab-containing regimens [13,15]. Notably, a high abundance of TAMs with an M2-like phenotype, characterized by CD163 expression, has been associated with poor prognosis, even in patients treated with rituximab [16]. Consequently, further investigation into the correlation between clinicopathological features, prognosis, and M2 TAMs is urgently required.

The aim of this study is to identify genes associated with M2 macrophage infiltration in DLBCL and develop a prognostic model to predict patient outcomes, stratifying individuals into high and low risk groups. Furthermore, we seek to assess the therapeutic sensitivity to various treatments, offering a theoretical basis for the development of novel therapeutic approaches for DLBCL.

#### 2. Materials and methods

#### 2.1. Patients and cohorts

Gene expression data (RNA-seq) from 481 DLBCL samples, along with clinical follow-up and clinicopathological information, were retrieved from The Cancer Genome Atlas (TCGA) using the TCGAbiolinks [17] R package in R software (version 4.2.2, https://www.r-project.org). Additional clinical and genetic subtypes data for DLBCL patients were retrieved from the supplementary files of the GDC DLBCL publication [3]. Additionally, gene expression data coupled with corresponding clinical information for 414 and 498 DLBCL patients were retrieved from the GSE10846 and GSE31312 datasets, respectively [4,18].

Gene expression levels, quantified as Transcripts Per Kilobase Million (TPM), were ascertained by leveraging the count2TPM function available in the IOBR R package [19]. For gene symbol annotation, the *Homo sapiens* GRCh38 annotation file was retrieved from Ensembl [20]. Data Preprocessing for Microarray: The Robust multi-array average (RMA) algorithm was employed to uniformly preprocess and normalize the raw array data [21].

### 2.2. Characterization of lymphoma immune microenvironment

The ESTIMATE algorithm was used to infer the proportions of immune and stromal cells in the samples, utilizing the 'estimate' package in R [22]. To assess the immune cell composition, we employed the CIBERSORT algorithm using the CIBERSORT R script v1.03 package in R software. CIBERSORT results were derived from the leukocyte signature matrix (LM22) and the reference gene matrix [23]. Only samples with a CIBERSORT p-value <0.05 were included in the analysis.

### 2.3. Gene expression correlation analysis

Correlation analysis was performed using gene expression data from NCICCR-DLBCL and M2 macrophage infiltration information from CIBERSORT. A co-occurrence network linking M2 macrophage infiltration to genes associated with it was constructed based on Pearson's correlation coefficients (|R| > 0.45) and a p-value threshold of p < 0.001.

#### 2.4. Enrichment analysis of biological functions

Biological pathway enrichment analysis was conducted using the 'clusterProfiler' [24] to examine genes associated with M2 macrophage infiltration. GO and KEGG pathway analyses were performed to investigate the biological processes and signaling pathways linked to M2 macrophage infiltration. Moreover, GSEA was performed using the expression profiles of all genes across the two subtypes. This analysis aimed to identify gene sets that were significantly enriched in specific subtypes or risk categories.

### 2.5. Construction of risk assessment model

A model for predicting outcomes associated with M2 macrophages was constructed through the application of Cox and LASSO regression methods within the training group. First, we performed a univariate regression analysis to determine genes related to M2 macrophages that have a significant correlation with survival results. Genes with a p-value <0.01 were considered potential candidates. LASSO analysis was applied to further narrow down the selection of key M2 macrophage-related genes. This analysis was

conducted using the 'glmnet' package in R.

The risk model was developed using the expression values (M) of each selected M2 macrophage gene and its coefficient ( $\beta$ ). Risk score =  $\sum_{n=1}^{j} (\beta j^* M j)$ , where j represents the index of selected genes. Based on the median risk score, DLBCL patients were categorized into low- and high-risk subgroups. Time-dependent receiver operating characteristic (ROC) curves were utilized to assess the predictive accuracy of the model. The NCICCR-DLBCL dataset was used as the training dataset, and external validation was conducted using two distinct cohorts, GSE10846 and GSE31312. The clinical characteristics of the training and validation cohorts are summarized in Table 1. A significance threshold of p < 0.05 was applied to all statistical analyses.

#### 2.6. Relationship between the clinical characteristics and M2 macrophage-related risk model

To evaluate the prognostic accuracy of the risk model within specific subgroups defined by clinical factors such as age, gender, Ann Arbor stage, Eastern Cooperative Oncology Group Performance Status, lactate dehydrogenase (LDH) levels, cell of origin (COO), and number of extranodal sites, we performed a comparative survival analysis across different risk groups within each clinical subgroup.

Additionally, to clarify the association between the risk model and clinical variables, we analyzed the distribution of risk scores among various clinical subgroups. This comparison was conducted using the 'ggpubr' package in R, which facilitated the visualization and interpretation of the relationships between the risk model and specific clinical characteristics.

#### 2.7. Identification of independent prognostic factors and development of a nomogram

In the training and validation datasets, we executed univariate and multivariate regression analyses to determine whether the risk score and clinical parameters independently predicted outcomes in DLBCL patients. By incorporating these prognostic factors, we performed a nomogram using the 'foreign' and 'survival' packages in R. The nomogram effectively assigned score points to each prognostic factor based on its contribution to overall survival (OS). The C-index was utilized to evaluate the accuracy of the nomogram. Calibration curves visually demonstrated the agreement between observed and predicted survival rates.

#### 2.8. Correlation of immune modulators with the M2 macrophage-associated prognostic model

Immune checkpoint inhibitors (ICIs) have shown promise in cancer treatment by blocking checkpoint proteins and promoting T cells to target and eliminate cancer cells [25]. In the context of B-cell lymphoma, previous studies have identified several immune checkpoint genes, such as PD-1, CD47, CD276, LAG3, HAVCR2, and CTLA-4, as potential therapeutic targets [26–33]. The Wilcoxon test was employed to evaluate the relationship between the risk score and the expression levels of these checkpoint molecules. This analysis aimed to clarify the possible influence of the M2 macrophage-related risk model on the tumor immune microenvironment and its potential role in shaping immunotherapy approaches.

## 2.9. Predict drug sensitivity

In order to evaluate the response to chemotherapy in patients with DLBCL, we employed the R package "pRRophetic" for our analysis [34]. This package employs ridge regression to predict drug sensitivity for individual samples. The predictive accuracy was evaluated using the GDSC (Genomics of Drug Sensitivity in Cancer) training dataset [35]. In this analysis, we aimed to predict the

**Table 1**Clinical and pathological characteristics of patients with DLBCL in this study.

	Training cohort  NCICCR (n = 234)	Validation cohort-1 $\overline{\text{GSE10846 (n = 305)}}$	$\frac{\text{Validation cohort-2}}{\text{GSE31312 (n} = 426)}$
Age, No. (%)			
> 60 years	118 (50)	159 (52)	247 (58)
≤60 years	116 (50)	146 (48)	179 (42)
Gender, No. (%)			
Male	139 (59)	171 (56)	243 (57)
Female	95 (41)	134 (44)	183 (43)
Subtype, No. (%)			
ABC	87 (37)	125 (41)	183 (42)
GCB	111 (48)	133 (44)	203 (48)
Unknown	36 (15)	67 (15)	40 (10)
Ann Arbor Stage, No. (%)			
I or II	109 (47)	144 (47)	200 (47)
III or IV	121 (52)	161 (53)	226 (53)
ECOG score, No. (%)			
<2	166 (71)	230 (75)	350 (82)
≥2	52 (22)	75 (25)	76 (18)
Unknown	16 (1)	_	_

Abbreviations: ECOG: Eastern Cooperative Oncology Group; GCB: germinal center B-cell-like lymphoma; ABC: activated B-cell-like lymphoma.

sensitivity of DLBCL patients to specific chemotherapeutic or target agents. By employing ridge regression and cross-validation techniques, we obtained accurate predictions of drug sensitivity for each sample. The GDSC training set served as a valuable resource for training and validating the prediction model.

#### 2.10. Validation results by single-cell RNA sequence (scRNA-seq) analysis

For the validation of our findings, we utilized scRNA-seq data retrieved from the heiDATA (https://heidata.uni-heidelberg.de). This dataset included three normal control samples and three DLBCL samples. The Seurat R package (v4.0.2) was employed for maintaining data integrity and conducting quality control [36]. Genes detected in three were removed from further analysis to improve the accuracy of the results.

Prior to further analysis, we applied several quality control filters to the libraries. Libraries with more than 5 % mitochondrial transcripts were excluded to reduce potential bias from damaged cells. In addition, libraries exhibiting an abnormal range of unique molecular identifiers (UMIs) suggestive of doublets, as well as those with fewer than 200 expressed genes, were also discarded. After data preprocessing, we normalized the expression data to a logarithmic scale using the 'NormalizeData' function. To standardize the data, we employed the "ScaleData" function. Next, we identified marker genes with significant differential expression by applying the following criteria: genes must be detected in at least 25 % of cells within the target cluster, have a Wilcoxon test p-value <0.05, and exhibit a minimum log fold change of 0.25. Visualization of gene expression levels was performed using FeaturePlot, DotPlot, and DoHeatmap. Using established classical markers, we annotated the resulting clusters as T cells (CD2, CD3D, CD3E, CD3G, TRAC), NK cells (NKG7, GNLY), B cells (CD19, MS4A1, CD79A), and macrophages (CD163, CD68, CD14).

#### 2.11. Validation results by immunohistochemistry

To validate the protein expression of genes in the M2 macrophage-related risk model across both DLBCL and normal tissues, we retrieved data from the Human Protein Atlas [37]. Using these IHC data, we assessed the protein expression profiles of the M2 macrophage-related risk model genes in DLBCL samples and their corresponding normal tissue counterparts. This further strengthened the robustness of our findings and provided additional evidence for the potential clinical significance of the identified genes.

#### 2.12. Statistical analysis

All statistical analyses in this study were performed using R software (version 4.2.2, https://www.r-project.org/). Continuous variables between two groups were compared using the independent Student's t-test, while the Wilcoxon rank-sum test was employed for non-normally distributed variables.

#### 3. Results

### 3.1. Elevated infiltration of M2 macrophages is linked to adverse prognoses

To investigate the association between M2 macrophages and the prognosis of DLBCL, we utilized the CIBERSORT algorithm to quantify the M2 macrophage infiltration in the NCICCR-DLBCL samples. Following this, DLBCL patients were stratified into two groups based on high and low M2 macrophage infiltration. Kaplan-Meier survival analysis demonstrated a significant survival difference between the high- and low-M2 macrophage subgroups (Fig. 1A), with patients in the low-M2 macrophage subgroup showing improved overall survival (Fig. 1A). These findings were further corroborated by the analysis of the GSE10846 and GSE31312 datasets, which consistently demonstrated that patients with high infiltration of M2 macrophages had significantly poorer overall survival compared to the low M2 macrophage content group (Fig. 1B and C; p < 0.001, p = 0.024).

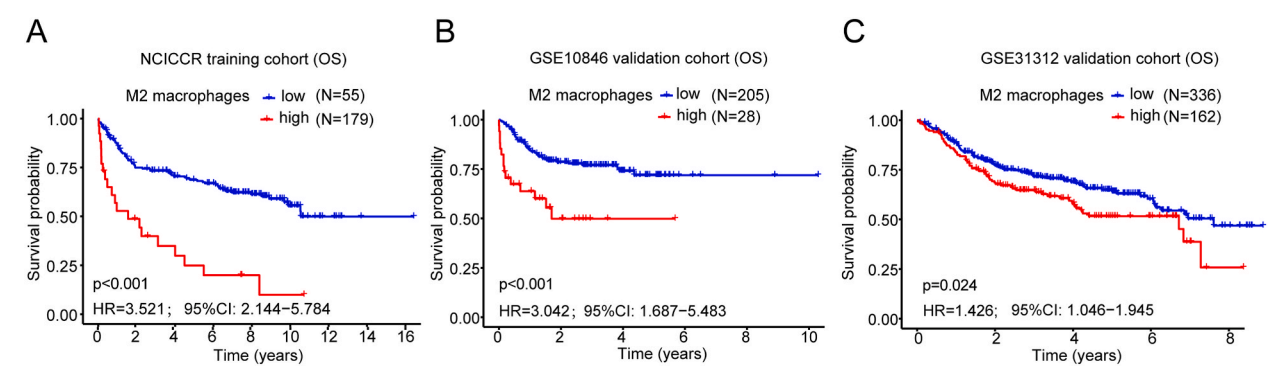


Fig. 1. The group with a high content of M2 macrophages exhibited significantly worse prognosis. (A) NCICCR training cohort; (B) GSE10846 validation cohort-1; (C) GSE31312 validation cohort-2.

#### 3.2. Identification of genes associated with M2 macrophage infiltration

To identify genes linked to M2 macrophage infiltration in DLBCL, we integrated the sequencing data from the NCICCR-DLBCL database with M2 macrophage infiltration data derived from CIBERSORT. A significance threshold of P < 0.001 and an absolute Pearson correlation coefficient (|R| > 0.45) were applied. Consequently, we identified 92 genes associated with M2 macrophage infiltration (Table S1). Fig. 2 illustrates the top six genes with the strongest correlations. Among the genes correlated with M2 macrophage infiltration, studies across various types of tumors have shown that MS4A4A is selectively expressed by tumor-associated macrophages [47]. Targeting MS4A4A may potentially enhance the efficacy of immune checkpoint inhibitors (ICIs) in DLBCL. CCL13, CCL23, and CCL18 are cytokine genes, and CCL18 plays a crucial role in the interaction of TAMs with neoplastic tumor cells [48]. Elevated CCL18 levels have been linked to poor prognosis in various cancers, including breast cancer, cutaneous T-cell lymphoma, and lung cancer [49–51].

### 3.3. Gene correlation analysis and exploration of potential underlying mechanisms

Utilizing the 92 identified genes, we generated a co-expression network diagram to showcase their complex interplay and connections (Fig. 3A). A correlation analysis was performed to examine gene relationships (Fig. 3B). We also carried out GO and KEGG pathway analyses based on these genes (Fig. 3C and D). The KEGG analysis highlighted significant alterations in pathways related to phagosome dynamics, complement regulation, coagulation cascades, and B cell receptor signaling. In the GO analysis, several biological pathways were notably impacted, including the response to external stimuli, activation of immune responses, leukocyte proliferation, and eosinophil migration. Moreover, there were distinct changes in cytological components, such as the secretory granule membrane, collagen trimer, and cytoplasmic vesicle lumen. Additionally, significant alterations in molecular functions were observed, particularly in immune receptor activity, immunoglobulin binding, chemokine activity, and chemokine receptor binding. These co-expressed genes potentially modulate M2 macrophage infiltration in DLBCL through the following mechanisms. The complement of phagosomes, coagulation cascades, and signaling pathways of the B cell receptor, as highlighted in the KEGG analysis, are also proposed as potential mechanisms through which M2 macrophages may facilitate tumor progression [45]. KEGG analysis has revealed a statistically significant association between changes in the Coronavirus disease (COVID-19) and M2 macrophage activity, implying that COVID-19 infection may potentially enhance M2 macrophage function, thereby influencing the development of DLBCL.

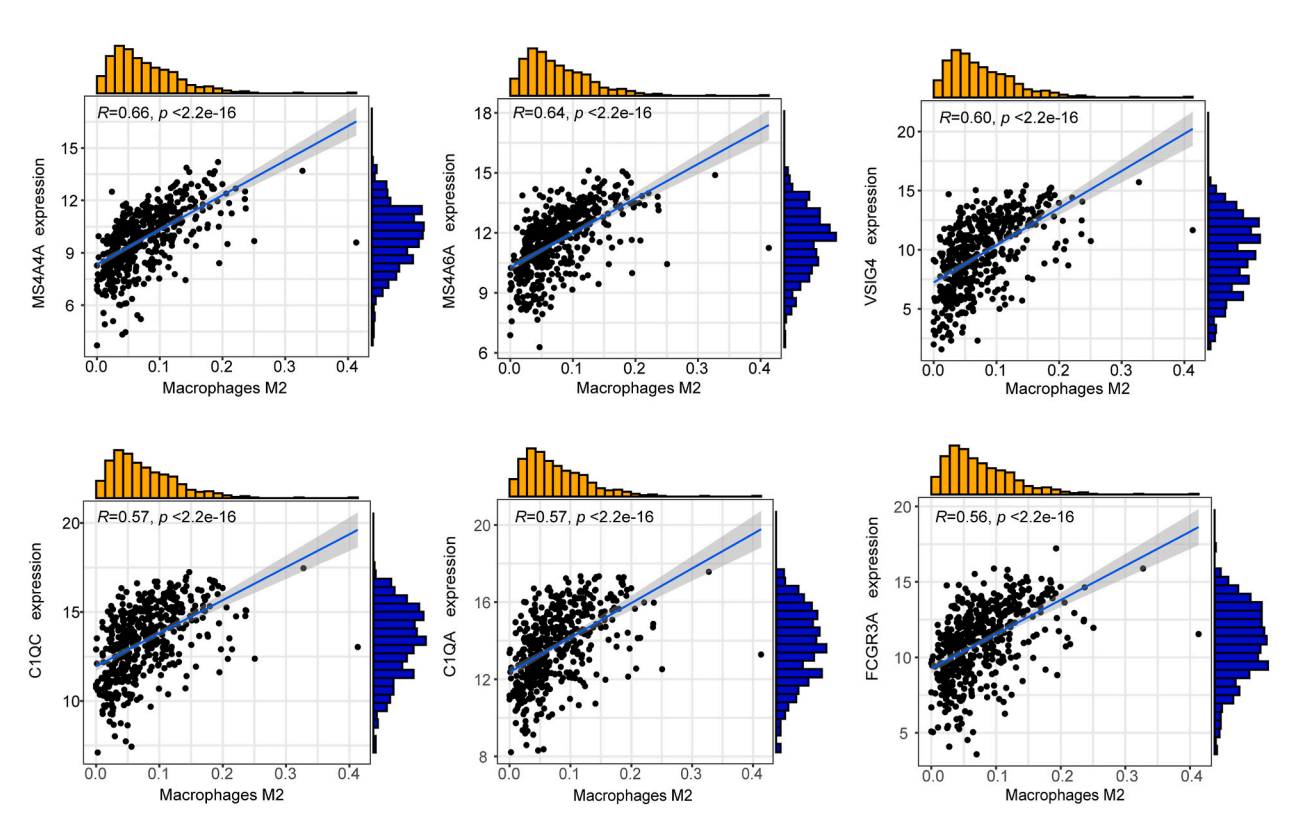


Fig. 2. Correlation maps of the top 6 genes associated with M2 macrophage infiltration.

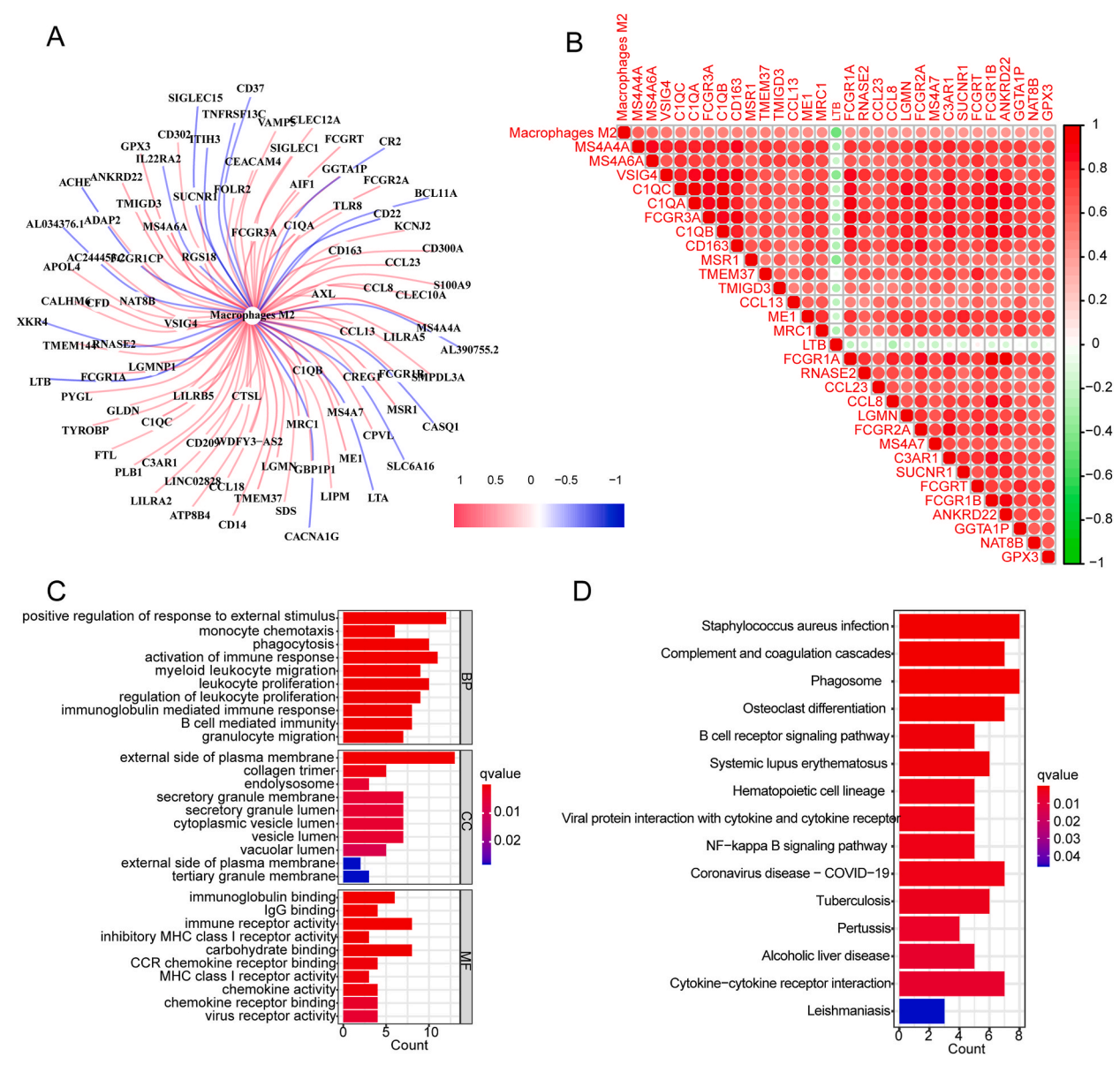
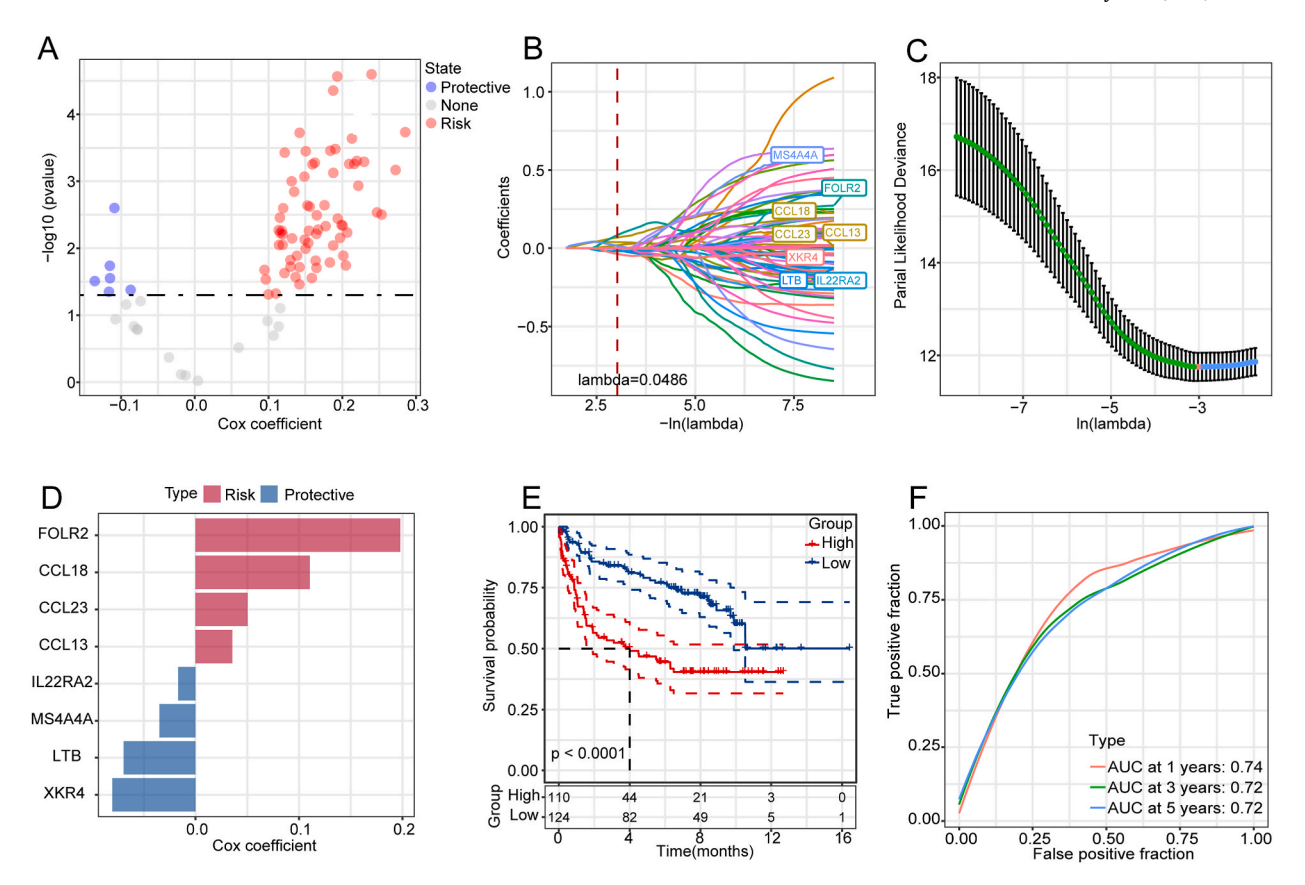


Fig. 3. Results of gene correlation, GO, and KEGG analyses. (A) Co-occurrence network between M2 macrophage infiltration and genes related to M2 macrophage infiltration; The red and blue linkages indicate the positive and negative correlations, respectively; (B) Results of correlation analysis; (C–D) Results of GO and KEGG analysis.

#### 3.4. Construction and validation of prediction models

In the training cohort (NCICCR-DLBCL dataset), we conducted univariate regression analysis using the gene expression profiles of 92 genes and survival data from DLBCL patients, identifying 66 prognostic genes (Fig. 4A). Next, LASSO Cox regression was employed to select the optimal subset of genes for the risk score model, ultimately identifying 8 M2 macrophage-related genes that formed the foundation of our prognostic signature in DLBCL (Fig. 4B–D). Risk score = (MS4A4A × -0.035) + (CCL13 × 0.036) + (LTB × -0.07) + (CCL23 × 0.05) + (CCL18 × 0.11) + (XKR4 × -0.08) + (IL22RA2 × -0.017) + (FOLR2 × -0.017). Patients were categorized into high-risk (n = 110) and low-risk (n = 124) groups based on the median risk score threshold. The survival outcomes were markedly poorer for the high-risk group compared to the low-risk group (p < 0.001, Fig. 4E). Time-dependent ROC curve analysis indicated strong predictive accuracy (AUC values: 1-year: 0.74, 3-year: 0.72, and 5-year: 0.72) (Fig. 4F). Similarly, the high-risk subgroup had markedly poorer prognoses than the low-risk subgroup (Fig. 5A–C; p < 0.001 for GSE10846; p < 0.05 for GSE31312). Additionally, the AUC values for the two independent validation cohorts varied between 0.67 and 0.84 (Fig. 5B–D), reinforcing the reliability and predictive accuracy of our model.



**Fig. 4.** Construction of an M2 macrophage-related prognostic model. (A) Univariate prognostic analysis results; (B) Lasso regression analysis results; (C) Cross-validation results; (D) Eight M2 macrophage-related prognostic model genes used to create our prognostic signature in DLBCL; (E) Survival analysis results in NCICCR training cohort; the dashed lines indicate the corresponding 95 % confidence intervals; (F) ROC curves and AUCs for 1, 3, and 5 years in the NCICCR training cohort.

Furthermore, we performed gene set enrichment analysis based on different risk scores. The high-risk group showed enrichment in pathways related to antigen processing and presentation, as well as the PPAR signaling pathway (Fig. S1). On the other hand, the low-risk group was predominantly associated with enriched pathways, including metabolism of ascorbate and aldarate, olfactory transduction, and metabolism of porphyrin and chlorophyll (Fig. S2).

## 3.5. Distribution of risk scores in various subtypes of DLBCL

DLBCLs of the activated B-cell-like subtype were overrepresented in the high-risk subgroup, whereas those of the germinal center B-cell-like subtype were predominantly found in the low-risk group (p=1.34e-14) (Fig. 6A–C). Schmitz et al. previously classified DLBCL into four major genetic subtypes, each demonstrating unique responses to immunochemotherapy: MCD, BN2, N1, and EZB. Different responses to immunochemotherapy were observed across these subtypes, with the BN2 and EZB groups demonstrating more favorable survival rates, whereas the MCD and N1 subtypes were correlated with worse outcomes. Specifically, the high-risk group contained a higher percentage of MCD patients, who are typically linked to poorer prognosis (Fig. 6B–D).

### 3.6. Predictive value of risk score on prognosis

A nomogram was constructed based on the NCICCR-DLBCL data, incorporating age, ECOG, and COO, all of which were found to be significant predictors of patient prognoses (Fig. 7A). Notably, the prognostic prediction using the risk score demonstrated excellent calibration for 1-, 3-, and 5-year prognoses, closely aligning with the actual prognoses of patients (Fig. 7B). Furthermore, the outcomes of both univariate and multivariate analyses demonstrated that the risk score exerts a independent influence on survival outcomes (Fig. 7C and D).

Additionally, we explored the impact of different clinical characteristics on the prognosis within each risk score subgroup. Notably, the survival advantage in the low-risk score group was particularly evident among patients with early Ann Arbor stages (I + II), age  $\leq$ 60, ECOG<2, fewer than 2 extranodal sites, and low IPI levels (Fig. 8A, B, C, D, E). Regarding the COO subgroups, high-risk scores in the ABC group correlated with worse survival outcomes, while the GCB group still demonstrated better prognosis regardless of risk

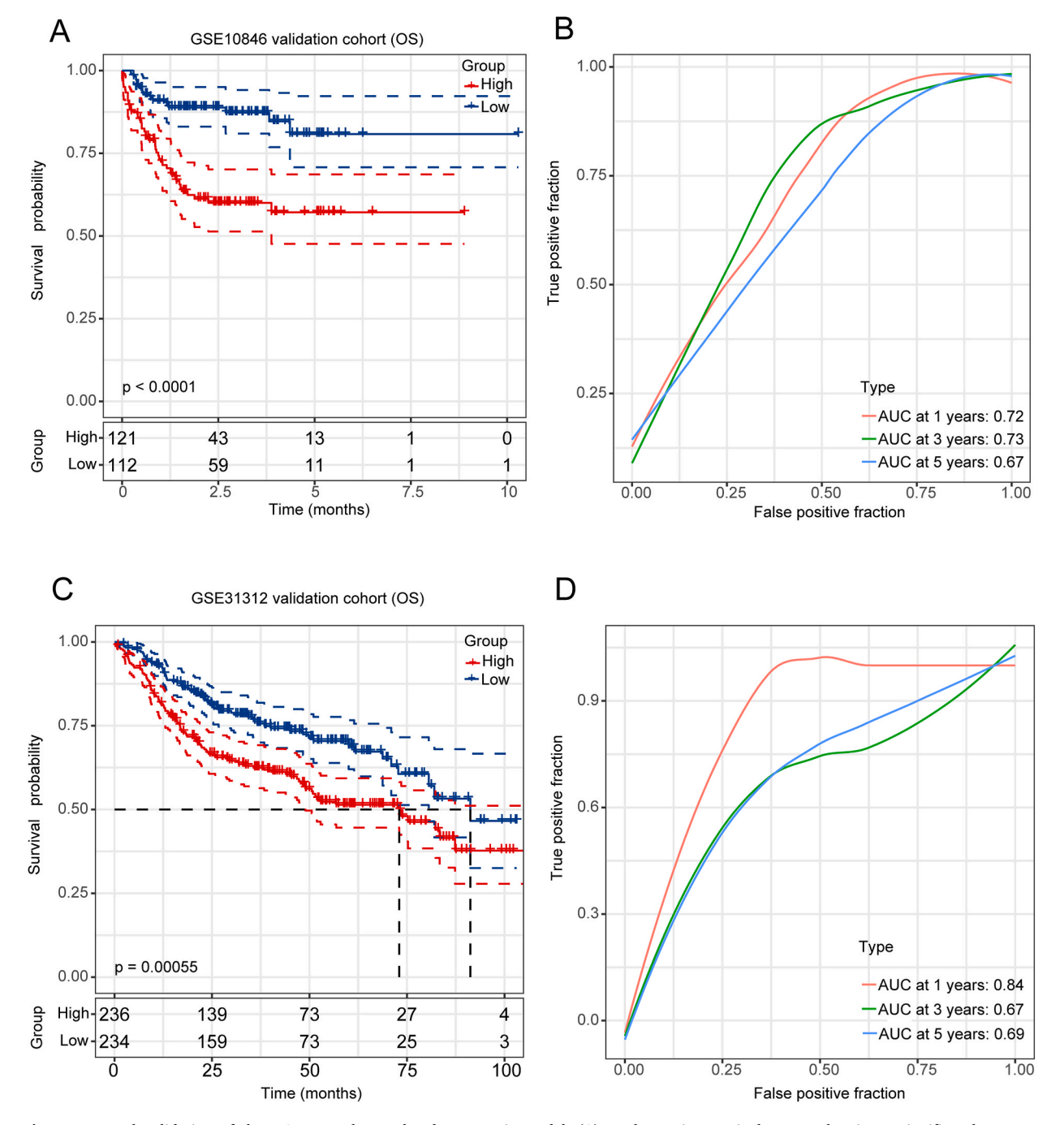


**Fig. 5.** External validation of the M2 macrophage-related prognostic model. (A) Kaplan-Meier survival curves showing a significantly worse prognosis for the high-risk group in the GSE10846 validation cohort; the dashed lines indicate the corresponding 95 % confidence intervals; (B) ROC curves and AUCs for 1, 3, and 5 years in the GSE10846 validation cohort; (C) Kaplan-Meier survival curves showing a significantly worse prognosis for the high-risk group in the GSE31312 validation cohort; (D) ROC curves and AUCs for 1, 3, and 5 years in the GSE31312 validation cohort.

score groups (Fig. 8F). The AUC of the risk score outperformed that of the IPI score in both the NCICCR training cohort and the GSE31312 validation cohort. (Fig. S3).

#### 3.7. M2 macrophage-related risk model and immunity

The results revealed a significantly higher infiltration of CD8 T cells, M1 and M2 macrophages, and monocytes in the high-risk group compared to the low-risk group (p < 0.01, Fig. 9A). Conversely, the low-risk group exhibited a notably higher frequency of

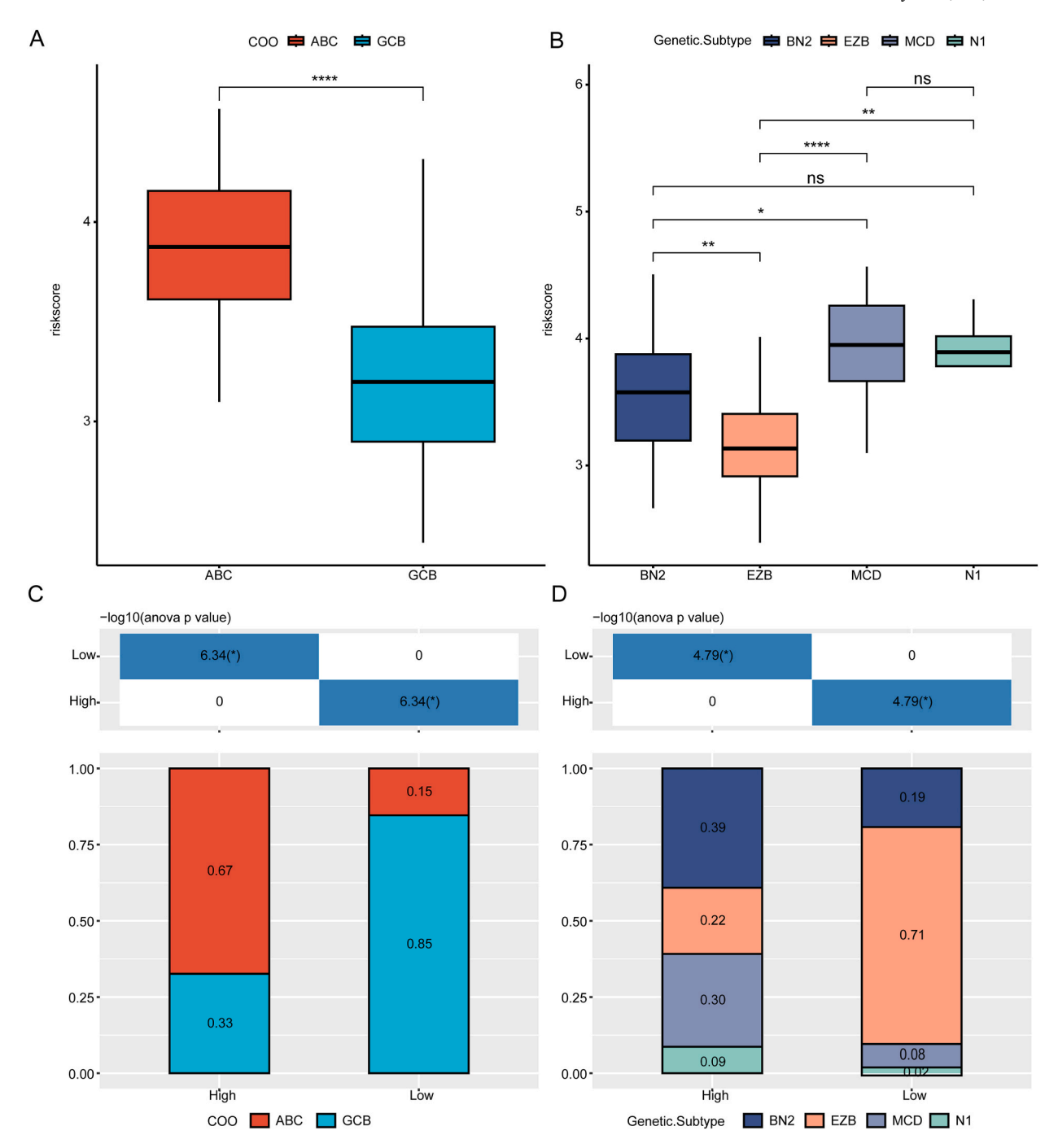


Fig. 6. Comparison of different risk scores in various subtypes of DLBCL. (A–B) Comparison of risk scores in various subtypes of DLBCL, with GCB representing germinal center B-cell-like lymphoma and ABC representing activated B-cell-like lymphoma. ns  $p \ge 0.05$ ; \*p < 0.05; \*p < 0.01; \*\*\*p < 0.001; \*\*\*p < 0.001; \*\*\*\*p < 0.0001. (C–D) Distribution of samples in different groups in the NCICCR cohort, showing the percentage of risk scores in each corresponding grouped sample. Different colors represent different subtypes of DLBCL. The table above presents the distribution of a certain subtype in any two risk groups and analyzes the p-value using the chi-square test.

M0 macrophages, memory B cells, and naïve B cells (p < 0.05). Furthermore, the expression of immune checkpoint markers (PD-1, PD-L1, PD-L2, CD47, CD276, LAG3, TIGIT, HAVCR2, and CTLA-4) was higher in the high-risk group (p < 0.01, Fig. 9B). Moreover, the high-risk group had elevated immune scores in contrast to the low-risk group (Fig. S4).

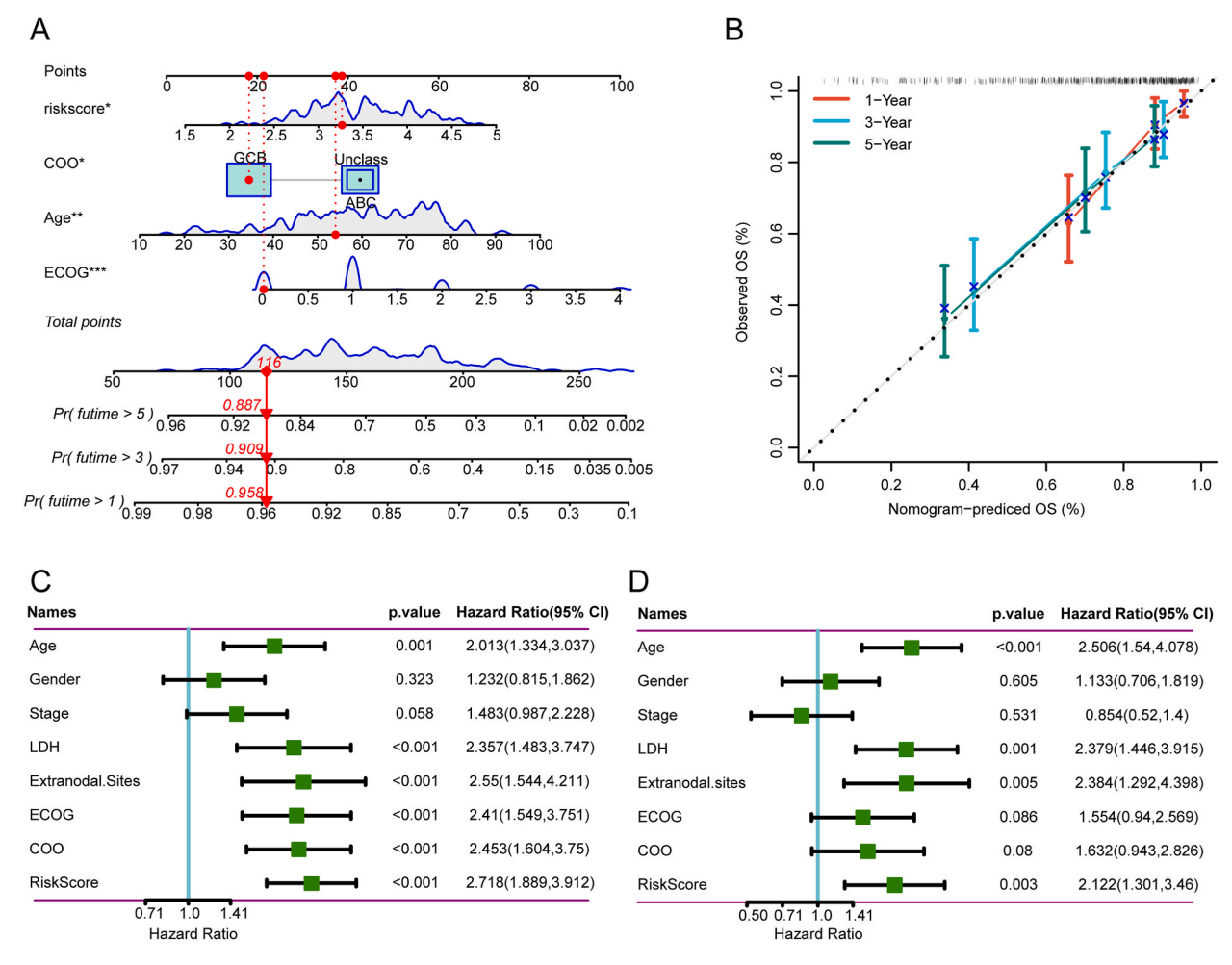


Fig. 7. Assessment of risk score on the prediction of patient prognosis. (A) Nomogram based on age, COO, risk score, and ECOG. ECOG represents Eastern Cooperative Oncology Group, and COO represents cell of origin. (B) Calibration curve of the nomogram, indicating agreement between predicted and observed survival in the model. (C–D) Results of univariate and multivariate analyses, demonstrating that the risk score is an independent factor influencing survival status over other indicators.

### 3.8. Verification of core M2 macrophage-related risk gene expression patterns using scRNA-seq and IHC analysis

To further confirm the cellular composition expressing the core M2 macrophage-related risk genes within the tumor microenvironment, we conducted scRNA-seq analysis using DLBCL data from the heiDATA database. The t-SNE analysis uncovered four distinct clusters of cells, which included B cells, monocyte-derived macrophages, NK cells, and T cells (Fig. 10A). Upon analyzing the expression pattern of the risk genes, we observed that MS4A4A, CCL18, IL22RA2, and FOLR2 were predominantly expressed in macrophages, while LTB showed a predominant expression in pan-leukocytes (Fig. 10B and C). Additionally, XKR4 was found to be expressed at low levels in NK cells, while FOLR2 and CCL23 were detected at low levels in B cells. The IHC results of protein expression for MS4A4A, CCL13, LTB, CCL23, CCL18, XKR4, IL22RA2, and FOLR2 obtained from the HPA database are displayed in Fig. S5.

#### 3.9. Screening for potential drugs with anti-cancer compounds

We utilized the GDSC database to assess their potential association with drug sensitivity. Drug sensitivity for each cancer cell line was quantified by the IC50 value, which represents the concentration required to inhibit cell growth by 50 %. A lower IC50 value indicates greater sensitivity to the drug. Considering the notably poorer prognoses observed in the high-risk group, we identified six drugs that demonstrated increased sensitivity in this cohort: Venetoclax, AZD7762 (a novel checkpoint kinase inhibitor), AZD6482, Bortezomib, Epirubicin, and Cyclophosphamide (Fig. 11). This analysis suggests that grouping patients based on their risk scores can aid in identifying DLBCL patients who may benefit more from these specific drugs.

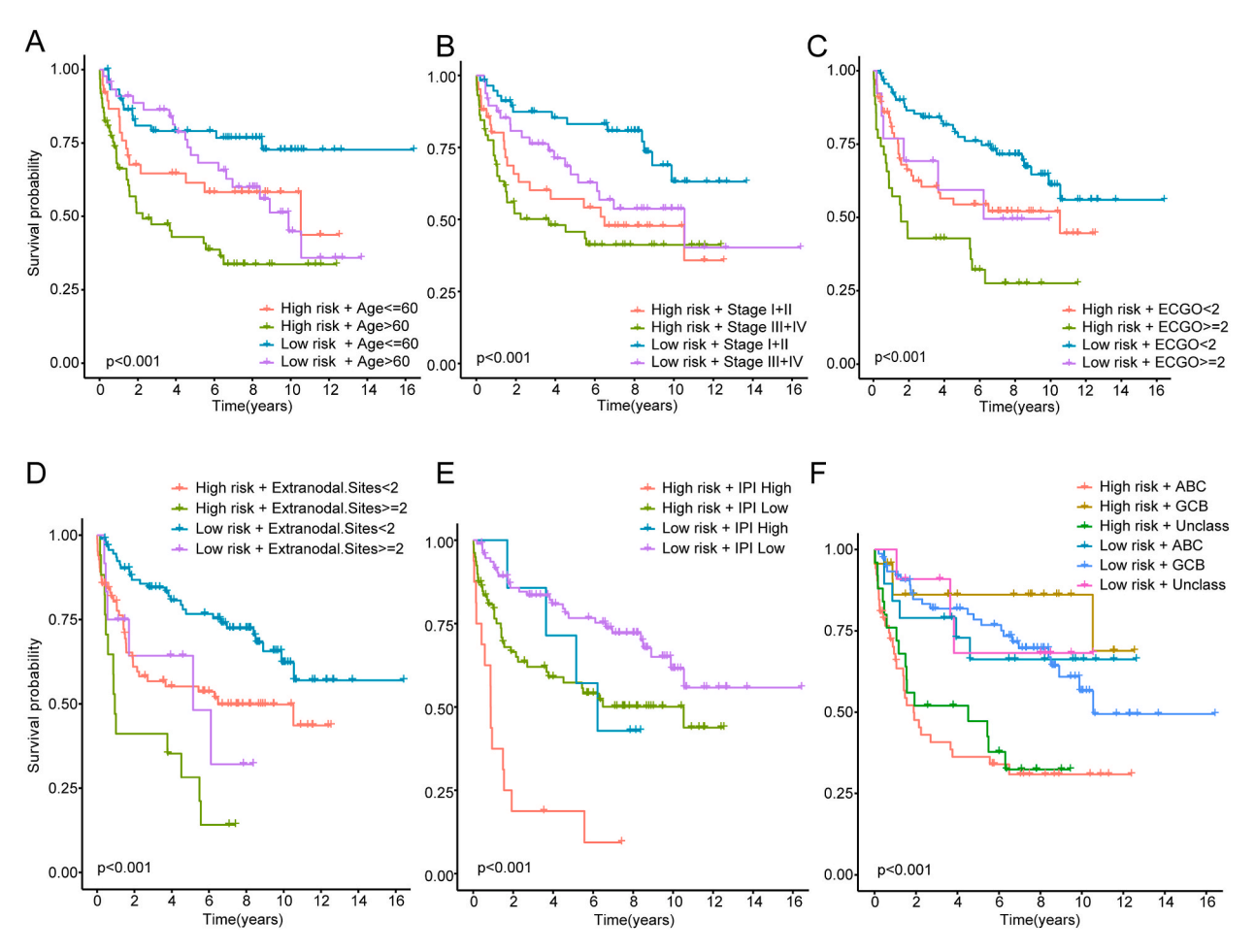


Fig. 8. Impact of different clinical characteristics on prognosis within each risk score subgroup. (A–F) Survival advantage among patients with different Ann Arbor stages, age, ECOG, extranodal sites, IPI levels, and COO subgroups. IPI represents International Prognostic Index, and COO represents cell of origin.

#### 4. Discussion

The involvement of tumor-associated macrophages in DLBCL has been widely investigated, with their presence linked to diverse prognostic outcomes, which are influenced by treatment protocols and the specific macrophage subtypes present [5]. Immunohistochemical studies have demonstrated that tumor-associated macrophage (TAM) markers, such as CD68 and CD163, are linked to poorer prognoses in DLBCL patients undergoing chemotherapy alone. However, the addition of rituximab to chemotherapy appears to improve outcomes, particularly in cases of de novo DLBCL [13]. In contrast, an elevated presence of tumor-associated M2 macrophages has been associated with poorer disease-free survival in de novo DLBCL patients treated with R-CHOP [38]. In this study, we sought to develop and validate a prognostic model specifically focused on M2 macrophage infiltration in DLBCL patients. The M2 macrophage-based prognostic model exhibited strong predictive accuracy for clinical outcomes, offering significant insights into the tumor microenvironment, activated signaling pathways, and patient responsiveness to chemotherapy and targeted therapies in DLBCL.

Previous studies have explored macrophage infiltration using various markers like CD68 or CD163 through immunohistochemistry assays. However, these studies yielded inconclusive results regarding the association between CD68 $^+$  and CD163 $^+$  TAM density and patient survival [5]. In our analysis, we applied the CIBERSORT to estimate the proportions and gene expression profiles of infiltrating M2 macrophages using publicly available datasets. Our findings consistently indicated that an increased presence of M2 macrophages correlated with reduced overall survival in both the NCICCR-DLBCL cohort and the validation cohorts GSE10846 and GSE31312 (p < 0.001). This is in line with a similar study by Chloé B. Steen et al., which reported that high levels of M2-like monocytes/macrophages in the gene expression profile were associated with unfavorable outcomes [39].

Subsequently, we identified genes co-expressed with M2 macrophages in the NCICCR-DLBCL cohort and investigated their influence on patient prognosis. The Gene Ontology (GO) analysis revealed that key molecular functions, such as the secretory granule membrane, collagen trimer, and cytoplasmic vesicle lumen, were primarily altered in the cellular components identified. These changes identified in the GO analysis represent potential mechanisms through which M2 macrophages may drive tumor progression.

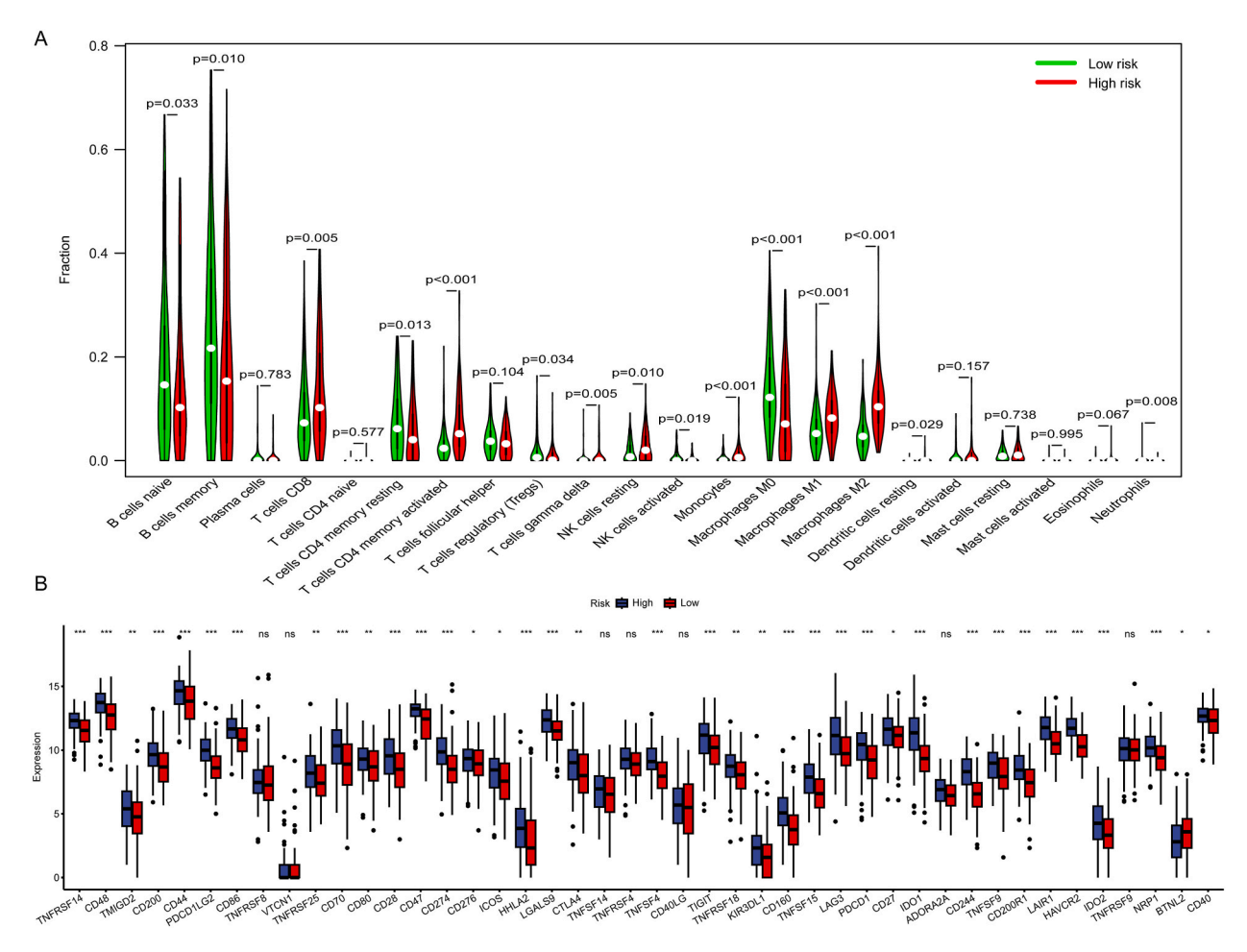


Fig. 9. Immune cell infiltration analysis. (A) Correlation of M2 macrophage-related prognostic model with immune cell infiltration. Green and red violins represent the low- and high-risk groups, respectively, and white points in the violin indicate median values. (B) Correlation between the M2 macrophage-related prognostic model and immune checkpoints. Blue and red boxplots represent the high- and low-risk groups, respectively.

Moreover, the activity of the MHC class I receptor was relatively diminished compared to other biological pathways. One of the primary mechanisms of immune evasion in DLBCL is the downregulation of MHC class I expression on the cell surface, a phenomenon that occurs in approximately 50 % of DLBCL cases [44]. This implies that M2 macrophages may influence the regulation of MHC class I expression, highlighting the need for further exploration. Additionally, pathways such as the phagosome pathway, coagulation cascades, and B cell receptor signaling, identified in the KEGG analysis, are potential mechanisms through which M2 macrophages could contribute to tumor progression [45]. Further research is essential to elucidate the detailed mechanisms, which will be a focus of our future work. Moreover, KEGG analysis has revealed a statistically significant association between changes in the Coronavirus disease (COVID-19) and M2 macrophage activity, implying that COVID-19 infection may potentially enhance M2 macrophage function, thereby influencing the development of DLBCL. This presents a novel avenue for research exploration. Using lasso regression analysis, we identified MS4A4A, CCL13, LTB, CCL23, CCL18, XKR4, IL22RA2, and FOLR2 as the genes required for model construction. The accuracy of the model was further confirmed through validation using data from the GEO database. The M2 macrophage-related prognostic model displayed robust predictive performance, effectively stratifying patients into high- and low-risk groups across all cohorts. Notably, the high-risk group was predominantly enriched in the activated B-cell-like (ABC) DLBCL and MCD LymphGen subtypes, reflecting different M2 macrophage prognosis subsets. Consistent with this, a previous study found that the S3 state of monocytes/macrophages, characterized by an M2-like expression profile and associated with poor prognosis, was most frequently observed in ABC DLBCL [39]. Previous indicated that both the BN2 and MCD subtypes are associated with poorer prognoses compared to other subtypes [40]. Specifically, the MCD-like subtype exhibits low expression of T cell signatures, suggesting a potentially less active immune response within the tumor microenvironment [40]. The study demonstrated that both MCD and BN2 subtypes exhibit a significantly greater proportion of high-risk patients. Previous research has established that the EZB subtype is related to GCB-DLBCL, which are associated with a favorable outcome [41-43]. Our findings showed a significant increase in the EZB subtype within the low-risk group. These findings showed the heterogeneity within DLBCL and the potential for subtype-specific therapeutic strategies. Additionally, the risk model remained effective after stratification based on various clinical factors. Our study demonstrated that

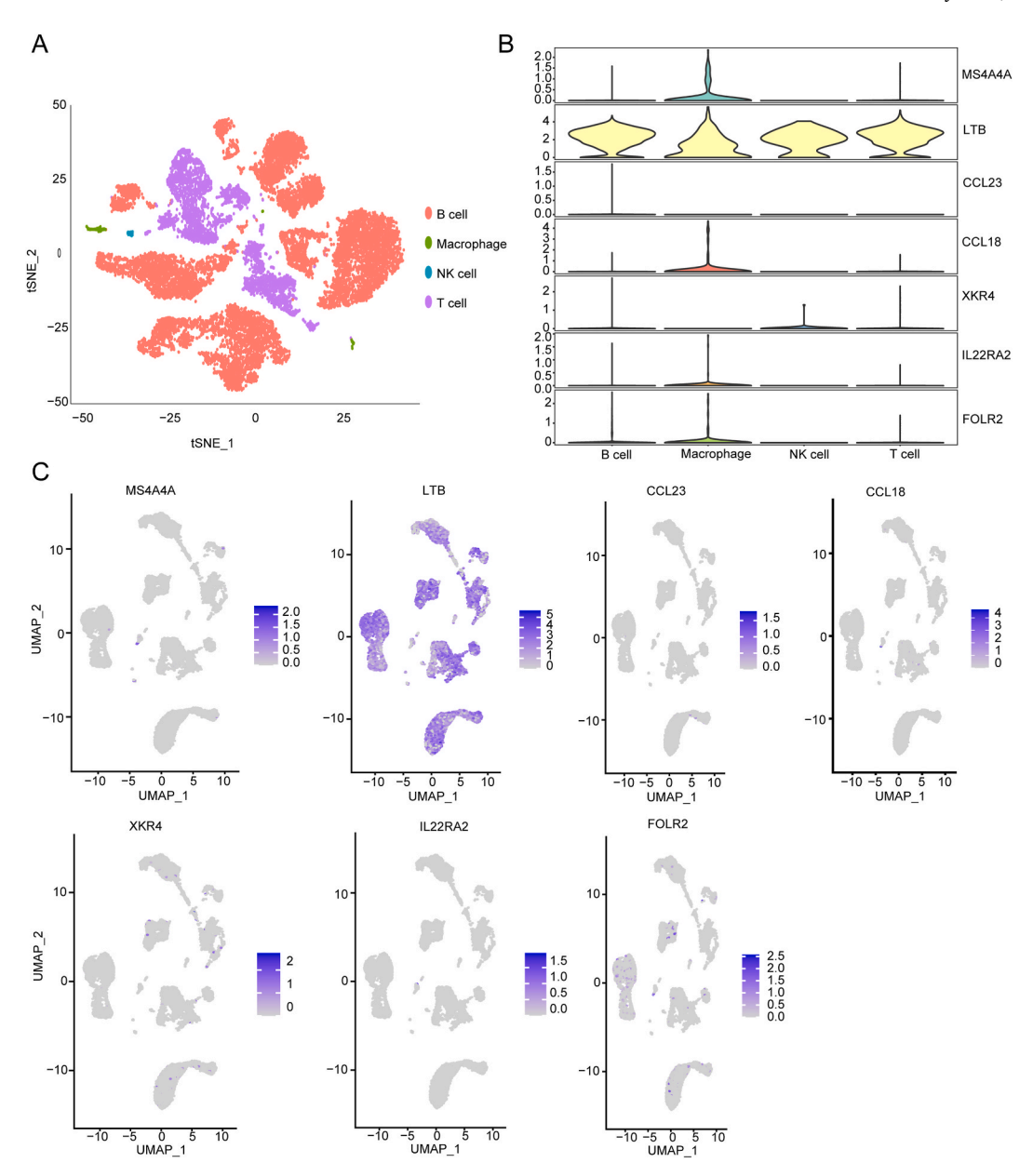


Fig. 10. scRNA-Seq reveals expression patterns of M2 macrophage-related risk model genes. (A) tSNE plots showing major cell subsets identified by 10×genomics. (B–C) Violin plots (B) and UMPA (C) plots showing different expression patterns of M2 macrophage-related risk model genes.

low-risk patients had significantly better prognoses in comparison to other groups, particularly among those with ECOG-PS $\geq$ 2, age $\leq$ 60, fewer than two extranodal sites, a low International Prognostic Index (IPI), and earlier disease stages.

The impact of the cell of origin (COO) status on DLBCL survival is well-established. Our study demonstrated that, while the prognoses of high- and low-risk germinal center B-cell-like (GCB) patients were comparable, low-risk activated B-cell-like (ABC) patients had significantly better outcomes compared to their high-risk counterparts. This finding may help to partially clarify the longer survival observed in patients with GCB DLBCL compared to those with ABC DLBCL. The M2 macrophage prognosis subsets appear to be influenced by COO, particularly in ABC DLBCL. Further studies are needed to explore the functional implications of these M2 macrophage prognostic subsets to verify our hypothesis.

Upon analyzing the roles of genes in the M2 macrophage risk model, we identified MS4A4A as a key macrophage marker, which has been linked to autoimmune disorders, including rheumatoid arthritis and cutaneous systemic sclerosis [46,47]. Recent studies across various tumor types have highlighted that MS4A4A is predominantly expressed by tumor-associated macrophages and is linked to poor clinical outcomes in cancer patients [48]. Targeting MS4A4A could potentially enhance the efficacy of immune checkpoint inhibitors (ICIs) in DLBCL. CCL13, CCL23, and CCL18 are cytokine genes, and CCL18 plays a crucial role in the interaction of TAMs with

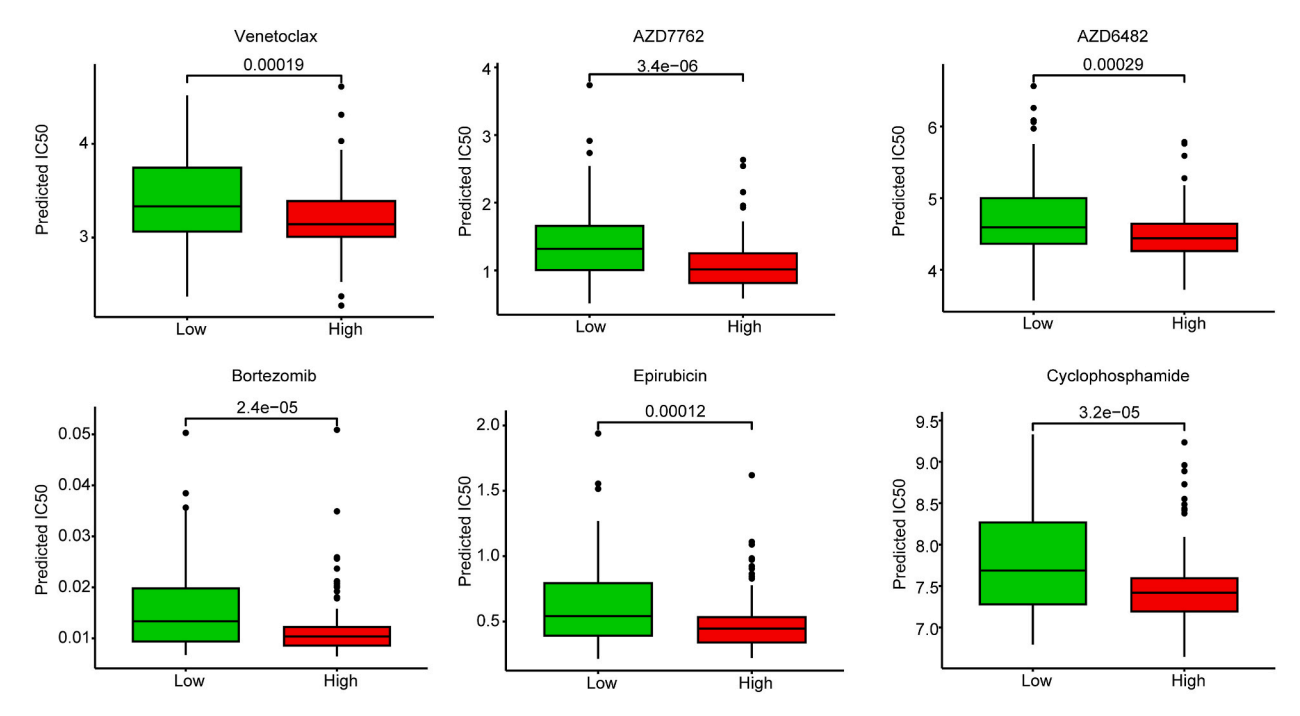


Fig. 11. Sensitivity analysis of chemotherapeutic and targeted drugs between different risk groups.

neoplastic tumor cells [49]. Elevated CCL18 levels have been correlated with poorer prognosis in various cancer types, such as breast cancer, cutaneous T-cell lymphoma, and lung cancer [50–52]. In contrast, IL22RA2 exhibits predominant expression in cells belonging to the myeloid lineage [53,54], whereas FOLR2+ macrophages have been linked to better survival outcomes in breast cancer patients [55]. Our analysis of DLBCL scRNA-seq data revealed that MS4A4A, CCL18, IL22RA2, and FOLR2 were predominantly expressed in macrophages, whereas LTB was mainly expressed in pan-leukocytes, and XKR4 was found at low levels in NK cells. The precise biological roles of the eight M2 macrophage-associated genes in the prognostic model for diffuse large B-cell lymphoma (DLBCL) are still not fully understood. Further investigation into the biological function, cell-specific expression, and topological analysis of these M2 macrophage risk model genes in DLBCL is warranted.

Our study also highlighted notable differences in immunological profiles and chemotherapeutic responses between the low and high risk subgroups. Wilcox test analysis indicated distinct immune cell infiltration patterns between these groups, with higher proportions of M1 and M2 macrophages, monocytes, CD4 memory-activated T cells, and CD8 T cells in the high-risk group. In contrast, the low-risk group exhibited relatively higher proportions of M0 macrophages, memory B cells, and naïve B cells. Additionally, immune checkpoint expression (PD-1, PD-L1, and CTLA-4) was significantly higher in the high-risk group. These findings indicate that the macrophages and CD8 T cells infiltrating the high-risk group may exhibit elevated levels of immune checkpoint expression, which could help explain the observed prognostic differences. Future studies should investigate whether immune checkpoint expression in different macrophage subsets contributes to therapeutic resistance to PD-1 blockade. Additionally, our observations indicated that the high-risk group had elevated stromal and immune scores, increased immune checkpoint gene expression, and reduced tumor purity. Elevated expression of immune checkpoint genes may foster an immunosuppressive microenvironment, facilitating tumor immune escape. GSEA analysis revealed that the low-risk group was predominantly enriched in metabolism-related pathways, whereas the high-risk group exhibited a significant enrichment in immune-related pathways.

Finally, leveraging the GDSC database, we predicted that the high-risk group may exhibit greater sensitivity to standard chemotherapy regimens compared to the low-risk group. Identifying patients who are less likely to respond to targeted therapies or chemotherapy could facilitate more tailored and effective treatment strategies. Notably, the drugs predicted by our risk model, such as Venetoclax, AZD7762 (a novel checkpoint kinase inhibitor), AZD6482, Bortezomib, Epirubicin, and Cyclophosphamide, all have potential utility in treating DLBCL. While the specific mechanisms of action of these small-molecule compounds require further investigation, our findings suggest their potential for tumor therapy, particularly among DLBCL patients, based on a combined score from eight genes, including MS4A4A, CCL18, LTB, IL22RA2, FOLR2, and XKR4.

Several limitations must be acknowledged in this study. The clinical data sourced from public databases were incomplete and lacked critical clinical information, highlighting the need for future prospective multicenter studies with larger sample sizes to further validate the accuracy and robustness of the M2 macrophage-related prognostic model. Moreover, functional experiments are necessary to further investigate the molecular mechanisms by which M2 macrophage-related genes impact the progression of DLBCL. The TCGA and GEO datasets might lack diversity in terms of patient demographics and geographic distribution. Consequently, future research involving prospective studies with more diverse validation cohorts will be essential to confirm and strengthen the robustness of our findings.

#### 5. Conclusion

In summary, this study identified M2 macrophage-related genes in DLBCL patients and successfully established and validated a robust M2 macrophage-related risk model for predicting overall survival in DLBCL. Our results suggest potential therapeutic targets for clinical practice and provide insights into the immune status of DLBCL. The findings contribute to a deeper understanding of M2 macrophage subset infiltration features and offer new strategies for personalized therapy. Further exploration of these findings and experimental validation will advance the field and potentially improve patient care.

#### CRediT authorship contribution statement

**Baoping Guo:** Writing – review & editing, Writing – original draft, Methodology, Formal analysis, Data curation. **Ying Duan:** Methodology, Formal analysis. **Hong Cen:** Writing – review & editing, Funding acquisition, Formal analysis, Data curation.

### **Ethics approval**

None.

#### Data availability statement

Data to support the findings of this study is available on reasonable request from the corresponding author. The datasets included in this study were obtain from the TCGA (https://portal.gdc.cancer.gov/) and GEO (http://www.ncbi.nlm.nih.gov/geo/).

#### **Funding**

This study was supported by Guangxi Natural Science Foundation (Grant No. 2023GXNSFDA026019) and Guangxi Zhuang Autonomous Region Health and Family Planning Commission (Grant No. Z-A20240705). The funders had no role in the study design, data analysis, written in the manuscript, or the decision to publish.

#### **Declaration of competing interest**

The authors declare that they have no known competing financial interests or personal relationships that could have appeared to influence the work reported in this paper.

## Acknowledgements

We would like to express our gratitude to authors for assistance with contribution.

## Appendix A. Supplementary data

Supplementary data to this article can be found online at https://doi.org/10.1016/j.heliyon.2024.e41007.

## References

- [1] G. Lenz, L.M. Staudt, Aggressive lymphomas, N. Engl. J. Med. 362 (15) (2010) 1417–1429, https://doi.org/10.1056/NEJMra0807082.
- [2] S. El Hussein, K.R.M. Shaw, F. Vega, Evolving insights into the genomic complexity and immune landscape of diffuse large B-cell lymphoma: opportunities for novel biomarkers, Mod. Pathol. 33 (12) (2020) 2422–2436, https://doi.org/10.1038/s41379-020-0616-y.
- [3] R. Schmitz, G.W. Wright, D.W. Huang, C.A. Johnson, J.D. Phelan, J.Q. Wang, et al., Genetics and pathogenesis of diffuse large B-cell lymphoma, N. Engl. J. Med. 378 (15) (2018) 1396–1407, https://doi.org/10.1056/NEJMoa1801445.
- [4] G. Lenz, G. Wright, S.S. Dave, W. Xiao, J. Powell, H. Zhao, et al., Stromal gene signatures in large-B-cell lymphomas, N. Engl. J. Med. 359 (22) (2008) 2313–2323, https://doi.org/10.1056/NEJMoa0802885.
- [5] M. Lin, S. Ma, L. Sun, Z. Qin, The prognostic value of tumor-associated macrophages detected by immunostaining in diffuse large B cell lymphoma: a meta-analysis, Front. Oncol. 12 (2022) 1094400, https://doi.org/10.3389/fonc.2022.1094400.
- [6] T. Takahara, S. Nakamura, T. Tsuzuki, A. Satou, The immunology of DLBCL, Cancers 15 (3) (2023), https://doi.org/10.3390/cancers15030835.
- [7] Z.Y. Xu-Monette, M. Xiao, Q.Y. Au, R. Padmanabhan, B. Xu, N. Hoe, et al., Immune profiling and quantitative analysis decipher the clinical role of immune-checkpoint expression in the tumor immune microenvironment of DLBCL, Cancer Immunol. Res. 7 (4) (2019) 644–657, https://doi.org/10.1158/2326-6066. CIR-18-0439.
- [8] M. Autio, S.K. Leivonen, O. Bruck, S. Mustjoki, J. Meszaros Jorgensen, M.L. Karjalainen-Lindsberg, et al., Immune cell constitution in the tumor microenvironment predicts the outcome in diffuse large B-cell lymphoma, Haematologica 106 (3) (2021) 718–729, https://doi.org/10.3324/haematol.2019.243626.
- [9] A. Sica, A. Mantovani, Macrophage plasticity and polarization: in vivo veritas, J. Clin. Invest. 122 (3) (2012) 787–795, https://doi.org/10.1172/JCI59643.
- [10] A. Mantovani, P. Allavena, F. Marchesi, C. Garlanda, Macrophages as tools and targets in cancer therapy, Nat. Rev. Drug Discov. 21 (11) (2022) 799–820, https://doi.org/10.1038/s41573-022-00520-5.

[11] Q.C. Cai, H. Liao, S.X. Lin, Y. Xia, X.X. Wang, Y. Gao, et al., High expression of tumor-infiltrating macrophages correlates with poor prognosis in patients with diffuse large B-cell lymphoma, Med. Oncol. 29 (4) (2012) 2317–2322, https://doi.org/10.1007/s12032-011-0123-6.

- [12] S.J. Nam, H. Go, J.H. Paik, T.M. Kim, D.S. Heo, C.W. Kim, et al., An increase of M2 macrophages predicts poor prognosis in patients with diffuse large B-cell lymphoma treated with rituximab, cyclophosphamide, doxorubicin, vincristine and prednisone, Leuk. Lymphoma 55 (11) (2014) 2466–2476.
- [13] S. Riihijarvi, I. Fiskvik, M. Taskinen, H. Vajavaara, M. Tikkala, O. Yri, et al., Prognostic influence of macrophages in patients with diffuse large B-cell lymphoma: a correlative study from a Nordic phase II trial, Haematologica 100 (2) (2015) 238–245, https://doi.org/10.3324/haematol.2014.113472.
- [14] C. Marinaccio, G. Ingravallo, F. Gaudio, T. Perrone, B. Nico, E. Maoirano, et al., Microvascular density, CD68 and tryptase expression in human diffuse large B-cell lymphoma, Leuk. Res. 38 (11) (2014) 1374–1377, https://doi.org/10.1016/j.leukres.2014.09.007.
- [15] M. Taskinen, M.L. Karjalainen-Lindsberg, H. Nyman, L.M. Eerola, S. Leppa, A high tumor-associated macrophage content predicts favorable outcome in follicular lymphoma patients treated with rituximab and cyclophosphamide-doxorubicin-vincristine-prednisone, Clin. Cancer Res. 13 (19) (2007) 5784–5789, https://doi.org/10.1158/1078-0432.CCR-07-0778.
- [16] Y.L. Li, Z.H. Shi, X. Wang, K.S. Gu, Z.M. Zhai, Tumor-associated macrophages predict prognosis in diffuse large B-cell lymphoma and correlation with peripheral absolute monocyte count, BMC Cancer 19 (1) (2019) 1049, https://doi.org/10.1186/s12885-019-6208-x.
- [17] A. Colaprico, T.C. Silva, C. Olsen, L. Garofano, C. Cava, D. Garolini, et al., TCGAbiolinks: an R/Bioconductor package for integrative analysis of TCGA data, Nucleic Acids Res. 44 (8) (2016) e71, https://doi.org/10.1093/nar/gkv1507.
- [18] E. Frei, C. Visco, Z.Y. Xu-Monette, S. Dirnhofer, K. Dybkaer, A. Orazi, et al., Addition of rituximab to chemotherapy overcomes the negative prognostic impact of cyclin E expression in diffuse large B-cell lymphoma, J. Clin. Pathol. 66 (11) (2013) 956–961, https://doi.org/10.1136/jclinpath-2013-201619.
- [19] D. Zeng, Z. Ye, R. Shen, G. Yu, J. Wu, Y. Xiong, et al., IOBR: multi-omics immuno-oncology biological research to decode tumor microenvironment and signatures, Front. Immunol. 12 (2021) 687975, https://doi.org/10.3389/fimmu.2021.687975.
- [20] K.L. Howe, P. Achuthan, J. Allen, J. Allen, J. Alvarez-Jarreta, M.R. Amode, et al., Ensembl 2021, Nucleic Acids Res. 49 (D1) (2021) D884–D891, https://doi.org/10.1093/nar/gkaa942.
- [21] C. Cheadle, M.P. Vawter, W.J. Freed, K.G. Becker, Analysis of microarray data using Z score transformation, J. Mol. Diagn. 5 (2) (2003) 73–81, https://doi.org/10.1016/S1525-1578(10)60455-2.
- [22] K. Yoshihara, M. Shahmoradgoli, E. Martinez, R. Vegesna, H. Kim, W. Torres-Garcia, et al., Inferring tumour purity and stromal and immune cell admixture from expression data, Nat. Commun. 4 (2013) 2612, https://doi.org/10.1038/ncomms3612.
- [23] A.M. Newman, C.L. Liu, M.R. Green, A.J. Gentles, W. Feng, Y. Xu, et al., Robust enumeration of cell subsets from tissue expression profiles, Nat. Methods 12 (5) (2015) 453–457, https://doi.org/10.1038/nmeth.3337.
- [24] G. Yu, L.G. Wang, Y. Han, Q.Y. He, clusterProfiler: an R package for comparing biological themes among gene clusters, OMICS 16 (5) (2012) 284–287, https://doi.org/10.1089/omi.2011.0118.
- [25] L. Galluzzi, J. Humeau, A. Buque, L. Zitvogel, G. Kroemer, Immunostimulation with chemotherapy in the era of immune checkpoint inhibitors, Nat. Rev. Clin. Oncol. 17 (12) (2020) 725–741, https://doi.org/10.1038/s41571-020-0413-z.
- [26] S.M. Ansell, S.A. Hurvitz, P.A. Koenig, B.R. LaPlant, B.F. Kabat, D. Fernando, et al., Phase I study of ipilimumab, an anti-CTLA-4 monoclonal antibody, in patients with relapsed and refractory B-cell non-Hodgkin lymphoma, Clin. Cancer Res. 15 (20) (2009) 6446–6453, https://doi.org/10.1158/1078-0432.CCR-09-1339.
- [27] Y.H. Lee, N. Martin-Orozco, P. Zheng, J. Li, P. Zhang, H. Tan, et al., Inhibition of the B7-H3 immune checkpoint limits tumor growth by enhancing cytotoxic lymphocyte function, Cell Res. 27 (8) (2017) 1034–1045, https://doi.org/10.1038/cr.2017.90.
- [28] R. Advani, I. Flinn, L. Popplewell, A. Forero, N.L. Bartlett, N. Ghosh, et al., CD47 blockade by Hu5F9-G4 and rituximab in non-hodgkin's lymphoma, N. Engl. J. Med. 379 (18) (2018) 1711–1721, https://doi.org/10.1056/NEJMoa1807315.
- [29] Z.Y. Xu-Monette, J. Zhou, K.H. Young, PD-1 expression and clinical PD-1 blockade in B-cell lymphomas, Blood 131 (1) (2018) 68–83, https://doi.org/10.1182/
- [30] Y. Jiang, J. Lin, J. Zhang, S. Lu, C. Wang, Y. Tong, Expression of co-inhibitory molecules B7-H4 and B7-H1 in Epstein-Barr virus positive diffuse large B-cell lymphoma and their roles in tumor invasion, Pathol. Res. Pract. 215 (12) (2019) 152684, https://doi.org/10.1016/j.prp.2019.152684.
- lymphoma and their roles in tumor invasion, Pathol. Res. Pract. 215 (12) (2019) 152684, https://doi.org/10.1016/j.prp.2019.152684. [31] H. Hatic, D. Sampat, G. Goyal, Immune checkpoint inhibitors in lymphoma: challenges and opportunities, Ann. Transl. Med. 9 (12) (2021) 1037, https://doi.org/10.21037/atm-20-6833.
- [32] K. Shimada, K. Yoshida, Y. Suzuki, C. Iriyama, Y. Inoue, M. Sanada, et al., Frequent genetic alterations in immune checkpoint-related genes in intravascular large B-cell lymphoma, Blood 137 (11) (2021) 1491–1502, https://doi.org/10.1182/blood.2020007245.
- [33] Y.H. Lee, H.J. Lee, H.C. Kim, Y. Lee, S.K. Nam, C. Hupperetz, et al., PD-1 and TIGIT downregulation distinctly affect the effector and early memory phenotypes of CD19-targeting CAR T cells, Mol. Ther. 30 (2) (2022) 579–592, https://doi.org/10.1016/j.ymthe.2021.10.004.
- [34] P. Geeleher, N. Cox, R.S. Huang, pRRophetic: an R package for prediction of clinical chemotherapeutic response from tumor gene expression levels, PLoS One 9 (9) (2014) e107468, https://doi.org/10.1371/journal.pone.0107468.
- [35] P. Geeleher, N.J. Cox, R.S. Huang, Clinical drug response can be predicted using baseline gene expression levels and in vitro drug sensitivity in cell lines, Genome Biol. 15 (3) (2014) R47, https://doi.org/10.1186/gb-2014-15-3-r47.
- [36] A. Butler, P. Hoffman, P. Smibert, E. Papalexi, R. Satija, Integrating single-cell transcriptomic data across different conditions, technologies, and species, Nat. Biotechnol. 36 (5) (2018) 411–420, https://doi.org/10.1038/nbt.4096.
- [37] M. Uhlen, L. Fagerberg, B.M. Hallstrom, C. Lindskog, P. Oksvold, A. Mardinoglu, et al., Proteomics. Tissue-based map of the human proteome, Science 347 (6220) (2015) 1260419, https://doi.org/10.1126/science.1260419.
- [38] F. Marchesi, M. Cirillo, A. Bianchi, M. Gately, O.M. Olimpieri, E. Cerchiara, et al., High density of CD68+/CD163+ tumour-associated macrophages (M2-TAM) at diagnosis is significantly correlated to unfavorable prognostic factors and to poor clinical outcomes in patients with diffuse large B-cell lymphoma, Hematol. Oncol. 33 (2) (2015) 110–112, https://doi.org/10.1002/hon.2142.
- [39] C.B. Steen, B.A. Luca, M.S. Esfahani, A. Azizi, B.J. Sworder, B.Y. Nabet, et al., The landscape of tumor cell states and ecosystems in diffuse large B cell lymphoma, Cancer Cell 39 (10) (2021) 1422–1437, https://doi.org/10.1016/j.ccell.2021.08.011, e10.
- [40] R. Shen, D. Fu, L. Dong, M.C. Zhang, Q. Shi, Z.Y. Shi, et al., Simplified algorithm for genetic subtyping in diffuse large B-cell lymphoma, Signal Transduct. Targeted Ther. 8 (1) (2023) 145, https://doi.org/10.1038/s41392-023-01358-y.
- [41] B. Chapuy, C. Stewart, C. Stewart, A. Kamburov, R.A. Redd, et al., Molecular subtypes of diffuse large B cell lymphoma are associated with distinct pathogenic mechanisms and outcomes, Nat. Med. 24 (5) (2018) 679–690, https://doi.org/10.1038/s41591-018-0016-8.
- [42] R. Schmitz, G.W. Wright, D.W. Huang, C.A. Johnson, J.D. Phelan, J.Q. Wang, et al., Genetics and pathogenesis of diffuse large B-cell lymphoma, N. Engl. J. Med. 378 (15) (2018) 1396–1407, https://doi.org/10.1056/NEJMoa1801445.
- [43] G.W. Wright, G.W. Wright, J.D. Phelan, Z.A. Coulibaly, S. Roulland, R.M. Young, et al., A probabilistic classification tool for genetic subtypes of diffuse large B cell lymphoma with therapeutic implications, Cancer Cell 37 (4) (2020) 551–568.e14, https://doi.org/10.1016/j.ccell.2020.03.015.
- [44] M. Fangazio, E. Ladewig, K. Gomez, L. Garcia-Ibanez, R. Kumar, J. Teruya-Feldstein, et al., Genetic mechanisms of HLA-I loss and immune escape in diffuse large B cell lymphoma, Proc. Natl. Acad. Sci. U.S.A. 118 (22) (2021) e2104504118, https://doi.org/10.1073/pnas.2104504118.
- [45] H. Wu, J. Feng, W. Zhong, W. Zhong, Z. Xiong, W. Huang, et al., Model for predicting immunotherapy based on M2 macrophage infiltration in TNBC, Front. Immunol. 14 (2023) 1151800, https://doi.org/10.3389/fimmu.2023.1151800.
- [46] I. Mattiola, F. Tomay, M. De Pizzol, R. Silva Gomes, B. Savino, T. Gulic, et al., The macrophage tetraspan MS4A4A enhances dectin-1-dependent NK cell-mediated resistance to metastasis, Nat. Immunol. 20 (8) (2019) 1012–1022, https://doi.org/10.1038/s41590-019-0417-y.
- [47] L.M. Rice, J. Ziemek, E.A. Stratton, S.R. McLaughlin, C.M. Padilla, A.L. Mathes, et al., A longitudinal biomarker for the extent of skin disease in patients with diffuse cutaneous systemic sclerosis, Arthritis Rheumatol. 67 (11) (2015) 3004–3015, https://doi.org/10.1002/art.39287.
- [48] Y. Li, Z. Shen, Z. Chai, Y. Zhan, Y. Zhang, Z. Liu, et al., Targeting MS4A4A on tumour-associated macrophages restores CD8+ T-cell-mediated antitumour immunity, Gut 72 (12) (2023) 2307–2320, https://doi.org/10.1136/gutjnl-2022-329147.

- [49] J. Korbecki, M. Olbromski, P. Dziegiel, CCL18 in the progression of cancer, Int. J. Mol. Sci. 21 (21) (2020) 7955, https://doi.org/10.3390/tjms21217955.
- [50] J.H. Sun, N. Fan, Y. Zhang, Correlation between serum level of chemokine (C-C motif) ligand 18 and poor prognosis in breast cancer, Genet. Mol. Res. 15 (3) (2016), https://doi.org/10.4238/gmr.15038632.
- T. Miyagaki, M. Sugaya, H. Suga, H. Ohmatsu, H. Fujita, Y. Asano, et al., Increased CCL18 expression in patients with cutaneous T-cell lymphoma: association
- with disease severity and prognosis, J. Eur. Acad. Dermatol. Venereol. 27 (1) (2013) e60–e67, https://doi.org/10.1111/j.1468-3083.2012.04495.x.

  [52] H. Huang, J. Li, W.J. Hu, C. Chen, H.Q. Luo, X.D. Tang, et al., The serum level of CC chemokine ligand 18 correlates with the prognosis of non-small cell lung cancer, Int. J. Biol. Markers 34 (2) (2019) 156-162, https://doi.org/10.1177/1724600819829758.
- [53] J.C. Martin, G. Beriou, M. Heslan, C. Chauvin, L. Utriainen, A. Aumeunier, et al., Interleukin-22 binding protein (IL-22BP) is constitutively expressed by a subset of conventional dendritic cells and is strongly induced by retinoic acid, Mucosal Immunol. 7 (1) (2014) 101-113, https://doi.org/10.1038/mi.2013.28
- [54] S. Huber, N. Gagliani, L.A. Zenewicz, F.J. Huber, L. Bosurgi, B. Hu, et al., IL-22BP is regulated by the inflammasome and modulates tumorigenesis in the intestine, Nature 491 (7423) (2012) 259-263, https://doi.org/10.1038/nature11535.
- [55] R. Nalio Ramos, Y. Missolo-Koussou, Y. Gerber-Ferder, C.P. Bromley, M. Bugatti, N.G. Nunez, et al., Tissue-resident FOLR2(+) macrophages associate with CD8( +) T cell infiltration in human breast cancer, Cell 185 (7) (2022) 1189-1207, https://doi.org/10.1016/j.cell.2022.02.02.1, e25.